Terahertz emission induced by optical beating in nanometer-length field-effect transistors

Philippe Nouvel, Jérémie Torres, Stéphane Blin, Hugues Marinchio, Christophe Palermo, Luca Varani, P. Shiktorov, Yevgeny Starikov, Vladimir Gruzinskis, Frederic Teppe, et al.

AIP | Journal of Applied Physics

Terahertz emission induced by optical beating in nanometer-length field-effect transistors

P. Nouvel, J. Torres, S. Blin, H. Marinchio, T. Laurent et al.

Citation: J. Appl. Phys. **111**, 103707 (2012); doi: 10.1063/1.4718445
View online: http://dx.doi.org/10.1063/1.4718445
View Table of Contents: http://jap.aip.org/resource/1/JAPIAU/v111/i10
Published by the American Institute of Physics.

Terahertz emission induced by optical beating in nanometer-length field-effect transistors

P. Nouvel,[1] J. Torres,[1,a)] S. Blin,[1] H. Marinchio,[1] T. Laurent,[1] C. Palermo,[1] L. Varani,[1] P. Shiktorov,[2] E. Starikov,[2] V. Gruzinskis,[2] F. Teppe,[3] Y. Roelens,[4] A. Shchepetov,[4] and S. Bollaert[4]
[1]*Institut d'Électronique du Sud-CNRS UMR 5214, TERALAB, Montpellier, France*
[2]*Semiconductor Physics Institute, A. Gostauto 11, Vilnius, Lithuania*
[3]*Laboratoire Charles Coulomb-CNRS UMR 5221, TERALAB, Montpellier, France*
[4]*Institut d'Electronique de Microelectronique et de Nanotechnologie, UMR 8520, Villeneuve d'Ascq cedex, France*

(Received 8 September 2011; accepted 27 April 2012; published online 21 May 2012)

We report on photo-induced terahertz radiation with a high spectral purity generated by a submicron sized InGaAs-based high-electron-mobility transistor. The emission peak is due to the electron-hole pairs photocreated in the transistor channel at the frequency of the beating of two cw-laser sources. The radiation frequency corresponds to the lowest fundamental plasma mode in the gated region of the transistor channel. The observed high emission quality factor at 200 K is interpreted as a result of stream-plasma instability in the two-dimensional electron gas whose appearance is emphasized by the reduction of the velocity relaxation rate with the temperature. © *2012 American Institute of Physics*. [http://dx.doi.org/10.1063/1.4718445]

I. INTRODUCTION

At the present time, high hopes of development of solid-state devices working at terahertz (THz) frequencies are connected to the use of modern electronic devices such as field-effect transistors (FETs) and high electron-mobility transistors (HEMTs). The distinctive features of these devices (high electron mobility, nonlinear current flow, two-dimensional (2D) plasma waves, etc.)[1–3] allow their use as detectors as well as generators of THz radiation. Recently, the possibility of both resonant and non-resonant detection of THz radiation based on these transistors was verified experimentally even at room temperature.[4,5] The use of FETs as THz sources has also been widely discussed in the literature.[6–9] In this case, the generation frequency is mainly controlled by the frequency of the 2D plasma oscillations excited in the channel. Such a situation can be realized when some instability, able to resonantly amplify the amplitude of the alternative component of the currents (ac-currents), develops in the transistor channel. These ac-currents excite the 2D plasma waves which play the role of source of electromagnetic radiation that will be emitted by the transistor into the surrounding space. The intensity of this emitted radiation is proportional to the squared amplitude of the ac-currents amplified by the instability. The Dyakonov-Shur instability[1] represents an example of such an amplification effect. However, the possibility to realize other kinds of stream-plasma instabilities,[10–13] as well as instabilities related to hot-carrier phenomena such as Gunn effect[14–16] or optical phonon emission assisted transit-time resonance,[17] is practically not discussed.

It should be emphasized that, in the case here considered, the physical nature of the instability is not a crucial factor. The instability merely amplifies the amplitude of the plasma waves of the transistor's channel without modifying significantly their spectrum. Usually, such a situation takes only place in a pre-threshold regime where the amplitude of the plasma waves sharply increases by approaching the threshold of instability. In this pre-threshold regime, relaxation processes become very long in time, while above the threshold, they are substantially changed into an exponential growth. The detailed physical nature of the instability will determine in which state the system will finally appear after crossing the threshold (oscillation frequency, linewidth, resonance quality, etc.).

The important peculiarity of the pre-threshold state is that the characteristics of the emitted radiation spectrum still depend on the physical nature of the source at the origin of the initial current fluctuations in the transistor channel. Usually, two kinds of such sources may be considered: the spontaneous—or internal—sources that describe the mechanism of thermal excitation and the induced—or external—sources when the initial fluctuations are excited from outside the device by some harmonic perturbation at frequency f. In the framework of a quasi-classical interpretation of the initial source as a generalized force, the formal description of the resulting emission spectrum is the same in both cases. However, the emission spectra and their intensity will have essential qualitative differences if the sources of fluctuations are internal or external. In the case of spontaneous excitation, it is generally assumed that the source is given by the internal thermal fluctuations appearing in the system (the so-called Langevin forces). In this case, the spectral intensity is independent of the frequency (classical case) or has a Planck distribution (quantum case).[18–21] With such a broadband source, the emitted radiation spectrum mimics the frequency dependence of the considered system (here the transistor channel) that is excited by the harmonic Langevin force at

a)jeremi.torres@ies.univ-montp2.fr.

the frequency f. In the absence of an instability, a spontaneous excitation simply initiates a broad-band emission noise spectrum containing resonances corresponding to the frequencies of eigen-plasma modes of the channel.[22]. Obviously, the obtention of a THz radiation of high spectral purity requires a high level of resonant amplification of the thermally excited plasma oscillations. This can only be realized when the instability threshold is overcome and the system operates in the regime of periodic self-oscillations. These oscillations will be characterized by frequencies corresponding to the eigenmodes of the plasma oscillations unperturbed by the instability. Such a transition through the threshold can be usually realized in submicron semiconductor structures when the free-carrier concentration is not sufficient to lead to the formation of particular structures like high-field domains, accumulation layers, etc.[17,23] Recent experiments devoted to the investigation of the spontaneous emission of THz radiations from AlGaN/GaN based HEMT structures[24] demonstrate the presence of a threshold for the appearance of the emission intensity. The authors have related this emission to the Dyakonov-Shur instability because the emission frequency coincides with the fundamental mode of 2D plasma waves. Nevertheless, the observed emission spectra are broadband; therefore, one can conclude that the instability development process did not reach in this experiment an amplification level sufficiently high to overcome the relaxation rate.

The main difference with respect to the induced mechanism of excitation of initial fluctuations is that the characteristics of the fluctuations source, such as its intensity and frequency spectrum, are not controlled now by internal processes but they are driven by external processes and, hence, they can be arbitrarily varied in a wide range. As a result, the radiation emission will take place only at frequencies where the external action excites ac-currents. The spectral width of the emission line will be linked to the frequency jitter in the source spectrum. In turn, the emission intensity dependence on the external source will be determined by internal characteristics of the system such as the set of resonant eigenfrequencies, the relaxation rates, and the amplification effects induced by the development of instabilities.

It is evident that, due to its nature, the induced excitation mechanism allows to obtain emitted radiation of high spectral purity that will be determined basically by the frequency stability of the external source of perturbation. In this case, an interesting possibility is to use as an external source an optical photoexcitation creating electron-hole pairs in the channel at the frequency of the beating of two cw-laser sources.[9]. The essence of the effect is that, under photoexcitation by two laser beams, it is possible to obtain a periodic generation of additional electron-hole pairs inside the transistor channel. If the photo-generated holes can quickly leave the channel (for instance crossing the gate contact), the concentration of the remaining photo-electrons in the channel will play the role of the external harmonic perturbation source responsible for the induced excitation of 2D-plasma waves. It is evident that the monochromaticity level of such a harmonic excitation will be only determined by the stability of the beating frequency of the two laser beams. Unfortunately, a direct experimental investigation of THz emission under photoexcitation of 2D plasma waves is still absent. Nevertheless, indirect experimental proofs evidencing the possibility of realization of such a high-monochromatic emission exist. As shown in Ref. 5, due to nonlinearities of the drain current in the transistor saturation region, it is possible to achieve the rectification of induced ac-currents. Under current-driven operation mode, this effect manifests itself as a resonant behavior of the dc-component of the source-to-drain voltage drop when the exciting frequency coincides with a frequency of the 2D eigen-plasma modes. Usually, this effect—also called self-detection or self-control—is used for the detection of photoexcited 2D plasma waves in the FET/HEMT channels.[25,26] By taking into account that the emission intensity and the rectification amplitude are proportional to the squared amplitude of photo-excited ac-oscillations and, hence, that their resonant dependences must be similar, the rectification effect can also be used for the self-control of the emitted radiation.

In the present communication, the results of direct measurements of emission of THz radiations caused by the photoexcitation of 2D plasma waves in InGaAs HEMT channels are presented for the first time. A comparison with results of the accompanying self-detection of the excitation of 2D plasma waves based on rectification effect is performed. Experimental results are also compared with the numerical results obtained using a hydrodynamic model.

II. EXPERIMENTAL CONFIGURATION

The experimental setup (see Fig. 1) repeats essentially that described in details in Refs. 27 and 28, and uses two commercially available distributed feedback (DFB) continuous-waves-lasers. Their central wavelengths of emission are $\lambda_1 = 1540.56\,\text{nm}$ and $\lambda_2 = 1542.54\,\text{nm}$ and exhibit a short-term spectral width of 2 MHz. Each laser (Power ≈ 10 mW) can be tuned over a range of approximately $\pm 1.5\,\text{nm}$ by changing the temperature (i.e., by varying the current in the Peltier stage). Their mixing, in a 2×2 polarization-

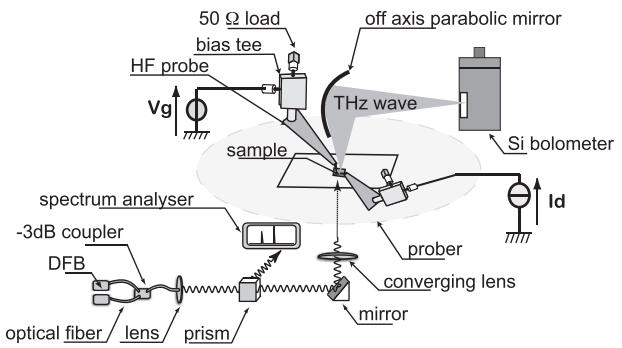

FIG. 1. Experimental configuration scheme. A tunable optical beating in the range 0.3-0.5 THz is produced by the spatial superposition of two cw-lasers at 1.55 μm (DFB). Using optical elements (lens, prism, mirror), the beating is focused onto the HEMT's channel (sample) while its stability is controlled by a spectrum analyser. The transistor is biased, using HF probes and 50 Ω loads, with constant voltage V_g between gate and source electrodes and constant current I_d at the drain electrode. The emitted radiation is collected by an off axis parabolic mirror and its intensity is measured by a 4 K-Si bolometer.

maintaining −3 dB coupler, produces a tunable optical beating in the range 0.3–0.5 THz. The uncertainty in the beating frequency (which is lower than 10 GHz) is estimated by measuring the fluctuations in time of the frequency of each laser with an optical spectrum-analyzer. Additionally, the new setup includes (i) the system of THz emission detection and (ii) the sample cooling system. The THz field emitted by the samples is collected by a 2-in. off-axis-parabolic mirror and focused inside a 4 K Si-bolometer placed close to the mirror. The temperature is decreased by connecting the sample substrate with thermal transfer ribbons immersed into a nitrogen bath. The temperature of the sample is monitored using a thermocouple. To avoid the formation of ice on the HEMT-top-facet, the experiment is made under a helium flow. Experiments were performed on HEMTs from InP technology with a gate-length value $L_g = 50$ nm. More detailed description of HEMT layers can be found in Ref. 26.

III. EXPERIMENTAL RESULTS

The main experimental results are presented in Figs. 2–4 which indicate three specific features of the considered phenomena.

A. Static source-to-drain current-voltage characteristics

The characteristics of the HEMT for a 50 nm gate length with a width of $W = 50\,\mu$m and a threshold voltage $U_{th} \approx -350$ mV are presented in Fig. 2. The gate potential U_g varied from −300 mV to 0 mV with 100 mV step. Solid and dotted lines correspond, respectively, to 300 K and 200 K lattice temperatures. The HEMT exhibits the typical current-voltage relation behavior $J_{sd}(U_{sd}, U_g)$ of source-to-drain current governed by source-to-drain and gate potentials. With decrease of the lattice temperature from 300 to 200 K, an increase of J_{sd} up to 10%–15% takes place reaching a maximum value at $U_g \to 0$ V. Such an increase of $J_{sd}(U_{sd}, U_g)$ agrees well with the change of free-carrier mobility in the HEMT channel. Estimations of the mobility change based on the IV-relation at low values of U_{sd} and $U_g \approx 0$ V give about a 10%–15% increase in going from 300 K to 200 K. Note that these IV-relations are independent of the operation regime of the source-to-drain circuit when (i) either the voltage-driven operation governed by variations of U_{sd} or (ii) the current-driven operation governed by the current J_{sd} fixed in external circuit are used.

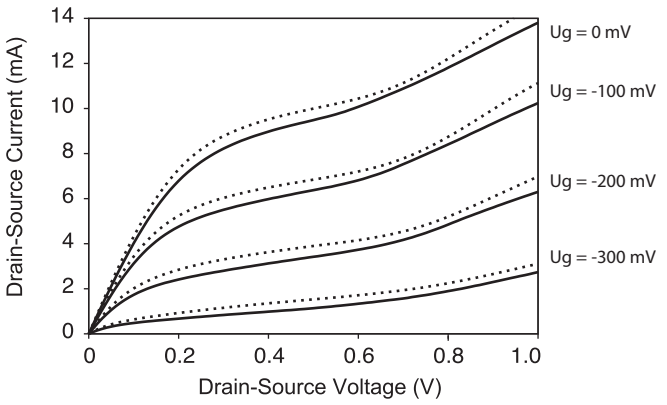

FIG. 2. Output characteristics at 300 K (solid lines) and at 200 K (dotted lines) for a 50 nm gate-length transistor with a width $W = 50\,\mu$m. The applied gate voltages are reported on the right side of the figure.

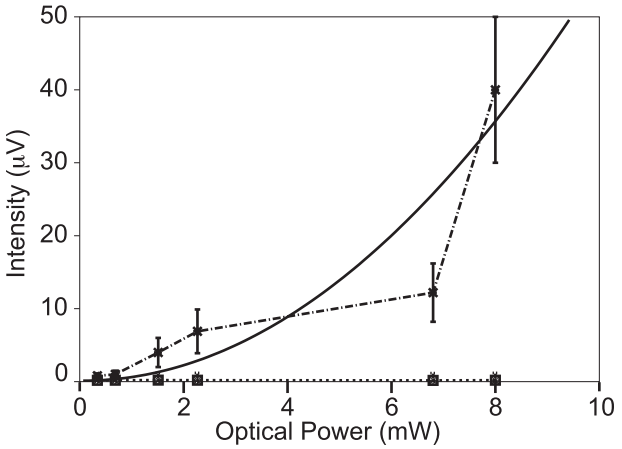

FIG. 3. Beam intensity emitted by the HEMTs and measured by a Si-bolometer at 200 K as a function of the power of the optical beating photoexcitation. Dashed lines: $f = f_0$ and dotted lines (coinciding practically with the horizontal axis): $f = f_0 \pm 10$ GHz. Solid lines are quadratic fits of the experimental results corresponding to the dashed lines.

B. Radiation emission from HEMT

In the absence of an external excitation, the experiment does not show any manifestation of radiation emission from

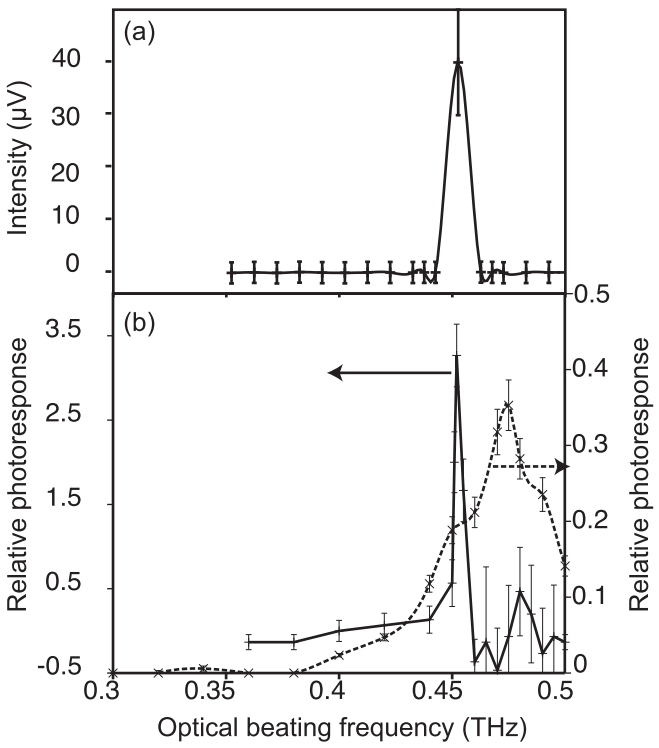

FIG. 4. (a) Spectral response of the THz beam measured by a Si-bolometer as a function of the optical beating frequency at 200 K. The solid line is a guide for the eyes. (b) Measured relative photoresponse versus the optical beating frequency ($U_g = -0.2$ V, $I_{sd} = 4$ mA at T = 300 K (dotted line) and at 200 K (solid line). Error-bars are experimental data joined by eye guidelines.

HEMTs related to the self-excitation of plasma waves as predicted in Ref. 1. A sharp resonant growth of the bolometer response was observed only under stimulated photoexcitation at $T = 200\,\mathrm{K}$ at values of the voltage drop between source-drain contacts $U_{sd} \sim 0.4 - 0.6\,\mathrm{V}$ and at a gate voltage $U_g \geq -0.2\,\mathrm{V}$ (Fig. 3). In this case, the beating frequency was close (with an accuracy of $\pm 10\,\mathrm{GHz}$) to the frequency of the first harmonic of excited plasma waves in the HEMT channel. In our case, this resonant frequency is equal to $f_0 = 0.455$ THz (see Ref. 27 for a more detailed explanation). As follows from Fig. 3, a sharp resonant emission of radiation in the frequency range $f_0 \pm 10$ GHz appears. It should be stressed that the bolometer response dependence on the pumping power is non-linear. With the increase of the beating frequency deviation from the resonant frequencies f_0 more than 10 GHz, the bolometer response signal went back to the thermal noise level. The minimum frequency step of 10 GHz is dictated by the frequency resolution realized in the beating experiments. The resonant emission takes place only if the transistors are biased under saturation of the static IV-curves (see Fig. 2), that is, at $U_{sd} \geq 0.2$ V. For smaller values of U_{sd}, the bolometer response remained within the thermal noise. Let us stress that, under induced excitation, the emission line-width is conditioned by the uncertainty of the excitation source. In these experiments, the uncertainty is not changed when the beating frequency changes and remains at the level of 10 GHz. This allows us to state that the results presented in Fig. 3 evidence that the emission intensity at $T = 200\,\mathrm{K}$ has a sharp resonant behavior in the frequency region corresponding to the excitation of the 2D plasma wave fundamental mode. Figure 4(a) shows the spectral response of the THz beam measured by the Si-bolometer at 200 K as a function of the optical beating frequency for the same transistor. As no emission is measured when the beating frequency varies of more than 10 GHz with respect to the frequency of the fundamental mode, we can state that the resonance full width at half maximum (FWHM) is not greater than 10 GHz.

C. Rectification of induced ac currents in HEMT channel

Due to the nonlinear character of the current flow in HEMT channels, it is possible to realize a self-control of the induced plasma wave intensity by measuring, under fixed drain current regime, the dc component of the source-drain voltage drop U_{sd} as a function of the external signal frequency f. As it was shown in Refs. 29 and 30, the resonant dependence on the beating frequency of the amplitudes of both the ac and the dc components of the drain-to-source voltage drop as well as of the ac-current in the channel are identical and are practically characterized by the same FWHM. Therefore, the experimentally obtained resonant behavior of the dc component of the drain-to-source voltage drop (i.e., the photoresponse) will also describe the emission intensity spectrum. Figure 4(b) illustrates the dependence of the relative magnitude of such a photoresponse R_f

$$R_f = \frac{U_{sd}(f) - \bar{U}_{sd}}{\bar{U}_{sd}}, \tag{1}$$

where $U_{sd}(f)$ is the source-drain voltage at the beating frequency f, while $\bar{U}_{sd}$ is the source-drain voltage drop at $f = 0$. Here dotted and solid lines correspond to measurements performed at 300 and 200 K, respectively, and were obtained for the maximum pumping power of 8 mW provided by the laser system. As follows from Fig. 4(b), the self-detection has a resonant character with a peak at frequencies $f_0 = 0.475$ and 0.455 THz at 300 and 200 K, respectively. Let us note that at $T = 200\,\mathrm{K}$, the resonant frequency of self-detection coincides exactly with the resonant frequency obtained in measurements of the emission intensity (see Fig. 3). As one can see from Fig. 4(b), the resonance line-width described by the FWHM sharply decreases from 40 to 5 GHz with temperature decrease from 300 to 200 K. Note that the estimation of the FWHM at $T = 200\,\mathrm{K}$ corresponds to the limiting value determined by the accuracy of the measured beating frequency; therefore, the FWHM real value can be even less than the above estimation. An important difference in the results of emission and self-detection is that at 300 K the bolometer does not detect any emission of radiation while the self-detection indicates a resonant photoexcitation of plasma waves at a slightly blue-shifted frequency $f_0 = 0.475$ THz (with respect to 0.455 THz). In our experiment, this slight frequency shift is not considered to be significant since it may be due to experimental artifacts such as ice formation at the level of the HF-probes or to the HEMT deterioration when decreasing the temperature that can slightly change the operating point of the device.

D. Discussion

Summarizing the experimental results, we can state that, in going from 300 to 200 K, (i) the static IV-relations are slightly changed showing about 10%–20% variation of the carrier-mobility in the HEMT channel, (ii) both techniques (the former one based on the resonant behavior of emission and the latter one on the rectification phenomenon) allow us to detect photoexcited plasma waves in the HEMT channel with eigenfrequencies of 2D plasma waves predicted by the theoretical model,[31] (iii) detection by using the rectification effect shows a photoexcitation of plasma waves at both 300 and 200 K with a resonance quality increase of about one order of magnitude, (iv) the direct radiation emission was measured only at 200 K while at 300 K it was absent, (v) the resonances of emission and rectification responses at 200 K are characterized by the same value of the FWHM < 10 GHz which is below the frequency resolution of the setup.

Most of these results can be interpreted in the framework of the theory of quasilinear response to an external perturbation, which assumes that the photoexcitation regime is linear and, hence, the amplitude of the ac-current, $j_d(f)$, appearing in the channel at the beating frequency f is proportional to the photoexcitation intensity P_0, i.e., $jd(f) \sim P_0$. In the framework of the linear theory, the experimentally measured signals $W(f)$ corresponding to the emission and rectification effects are related quadratically to the beating-induced ac-current amplitudes as $W(f) \sim |j_d(f)|^2$. As a consequence: (i) the emission power must have a quadratic dependence on the photo-excitation intensity. As follows

from Fig. 3, the experiment follows approximately this behavior. (ii) For both effects (emission and rectification), the dependence of the measured signal amplitudes on the beating frequency must be similar. The experimental results (see Figs. 3 and 4 as well as their comments in the text at 200 K) satisfy this condition. In both cases, the FWHM of the observed spectrum does not exceed 10 GHz. Probably, this value corresponds to the maximum frequency resolution of the experimental setup.

As it was noticed above, at 300 K the emission response was not observed. This also can be explained in the framework of the linear response. Following our estimations such a behavior is connected first to a not sufficient sensitivity of the setup used in the experiment for the detection of the emitted radiation. Indeed, since the frequency dependence of the emission and rectification responses must have similar behaviors, from Fig. 4 we can conclude that the emission power must decrease of about one order of magnitude in going from 200 to 300 K. For instance, by taking into account the sensitivity of the detection setup, at a level of ~15% with respect to the signal magnitude at 200 K, as it takes place in the experiment (see, e.g., vertical bars in Fig. 3), the emission response at 300 K cannot be extracted from the noise level.

At the same time, the origin of the sharp narrowing of the emission resonance with decrease of the lattice temperature cannot be explained in the framework of the linear response theory. Therefore, the following question appears: why a rather low decrease (about 10%–20%) of the velocity relaxation rate (i.e., of the mobility) in the HEMT channel in going from 300 to 200 K leads to a considerable enhancement of the resonance quality (about one order of magnitude) in measurements of the emitted and rectificated signals? In Sec. IV, we will show that such a behavior can be explained by the presence of a plasma instability in the stable situation when the amplification induced by the instability is still not sufficient to compensate the damping caused by the velocity relaxation rate.

IV. THEORETICAL ANALYSIS

In this section, we will analyze in detail the experimentally observed sharp narrowing of the plasma resonance lines in the emission and rectification response spectra when the FET/HEMT temperature decreases. Let us restrict ourselves to the simplest analytical model which allows, from one hand, to describe qualitatively and quantitatively the experimentally observed resonances of 2D plasma waves excited in FET/HEMT channels,[5] and from the other hand, to consider the development of Dyakonov-Shur instability of such waves which can appear due to the presence of carrier stream along the channel.[3,5]

A. Theoretical model

We assume that carrier transport in the transistor can take place only along the conductive channel from source to drain contacts, i.e., carrier flow in the transverse direction with respect to the channel is absent. This allows us to describe carrier transport as a one-dimensional (1D) process by using simple hydrodynamic (HD) equations

$$\frac{\partial n}{\partial t} + \frac{\partial nv}{\partial x} = G(t), \tag{2}$$

$$\frac{\partial v}{\partial t} + \frac{\partial}{\partial x}\left[\frac{v^2}{2} + \frac{e}{m^*}\varphi\right] + e\nu D\frac{\partial n}{\partial x} + v\nu = 0, \tag{3}$$

where n and v are the concentration and velocity of electrons in the channel, respectively, ν is the velocity relaxation rate, m^* the electron mass, D the longitudinal diffusion coefficient, and $G(t)$ is the electron photo-excitation generation term.

The self-consistent potential $\varphi(x)$ inside the channel is described by a 1D approximation of the 2D Poisson equation[22]

$$\varepsilon_c \frac{\partial^2}{\partial x^2}\varphi + \varepsilon_s \frac{U_g - \varphi}{d(x)\delta} = \frac{e}{\varepsilon_0}[n(x) - N_D(x)], \tag{4}$$

where δ is the channel width, U_g the gate potential, N_D the effective donor concentration in the channel, $d(x)$ the effective gate-to-channel distance. A dependence of $d(x)$ on the coordinate in the channel allows us to describe in the framework of Eq. (4) both gated regions where $d(x)$ has certain finite value and ungated regions where $d(x) \to \infty$ is supposed to tend to infinity.

When the channel width $\delta \to 0$ and the 2D free-carrier density in the channel $n^{2D}(x) = n(x)\delta$ keeps a finite value, Eq. (4) is reduced to the so called gradual channel approximation widely used in analytical models of FETs (Refs. 1–5)

$$\frac{U_g - \varphi(x)}{d} = \frac{e}{\epsilon_s \epsilon_0}[n^{2D}(x) - N^{2D}(x)], \tag{5}$$

where $N^{2D}(x) = N_D(x)\delta$. In essence, the gradual channel approximation of the Poisson equation given by Eq. (5) takes into account merely the gate-induced transverse Coulomb action on carriers in the channel. The longitudinal interaction of carriers in the channel which is responsible for the long-range effect of the Coulomb interaction (the spatial second-order derivative in Eq. (4)) is not accounted for in the framework of the gradual channel approximation.

It is worthwhile to stress limitations of the model based on Eqs. (2)–(4).

(i) Only one type of photo-generated carriers, i.e., electrons, is taken into account. The photo-generated holes contribution to the space charge and current along the channel is omitted by supposing that holes, just after photo-excitation, are practically immediately removed from the channel through the gate. The time dependence of the optical generation rate is taken in the form

$$G(t) = P_0[1 + \cos(2\pi ft)], \tag{6}$$

with f being the beating frequency and P_0 the photo-generation intensity.

(ii) Hot-carrier effects are not taken into account since the electron velocity relaxation rate ν is supposed to be constant along the channel and to be not dependent of the electrons local energy. This assumption allows

us to consider the development in FET/HEMT channels of mono-stream plasma instabilities only.

Under voltage driven operation, the system of Eqs. (2)–(4) is closed, thus allowing us to calculate various steady-state and transient characteristics. In the case of boundary conditions for Eq. (4), we have used potentials $\varphi(0)$ (usually equal to zero) and $\varphi(L)$ given in points $x = 0$ and $x = L$, respectively, where L is the channel total length.

Under current-driven operation one fixes the total current at the drain contact $j_{tot}(L) = const$. Since the total current consists of the sum of conduction and displacement currents, the requirement to keep constant the total current can be reformulated in terms of an additional equation for the time-evolution of the electric field at the drain contact as

$$\frac{\partial}{\partial t}E(L,t) = \frac{1}{\varepsilon_c \varepsilon_0}[j_{tot} - en(L,t)v(L,t)]. \quad (7)$$

In this case, Eq. (7) is solved in parallel with Eqs. (2) and (3). The boundary condition for the Poisson equation at the source contact remains the same ($\varphi(0)$), while the drain boundary condition is rewritten in terms of the electric field $E(L,t)$.

In our calculations, we assumed that the lattice temperature is of about T = 200 K and that the corresponding value of the velocity relaxation rate is of about $\nu = 2\,(\mathrm{ps})^{-1}$. Such estimations of the relaxation rate of the electron velocity in the channel near thermal equilibrium are based on Hall-measurements of the investigated here HEMTs and on MC simulations of bulk $In_{0.53}Ga_{0.47}As$ at different temperatures. The diffusion coefficient is calculated from the low-field mobility μ by using Einstein relation $D = kT\mu/e$.

B. *Numerical results*

As it was already mentioned, the above model can reproduce the classical Dyakonov-Shur instability of 2D plasma waves caused by mono-stream of carriers under the gate. Figures 5 show the time dependences of the source-to-drain voltages corresponding to conditions of progressive development of the Dyakonov-Shur instability associated with a small decrease of the electron velocity relaxation rates 1.9, 1.75, and 1.7 ps^{-1}, respectively. The simulated structure and the bias conditions correspond to the experimental ones. In these figures, the relaxation process to the stationary state have an oscillating character with a frequency corresponding to the main harmonics of 2D plasma waves excited in the gated regions of the channel. The main difference is related to which stationary state the system relaxes. In the case of $\nu \geq 1.75$ ps^{-1} (Fig. 5(a)), the relaxation process leads the system to a time-independent stationary state through damped oscillations (the usual dissipative process of an oscillator). The peculiarity of the relaxation process presented in Fig. 5(b) is that, in contrast to the previous case, a rather small decrease of the relaxation rate (about 10%) results in a considerable decrease of the system relaxation (approximately one order in magnitude).

A further decrease of the velocity relaxation rate, $\nu <$ 1.75 ps^{-1} (Fig. 5(c)), changes qualitatively the system state

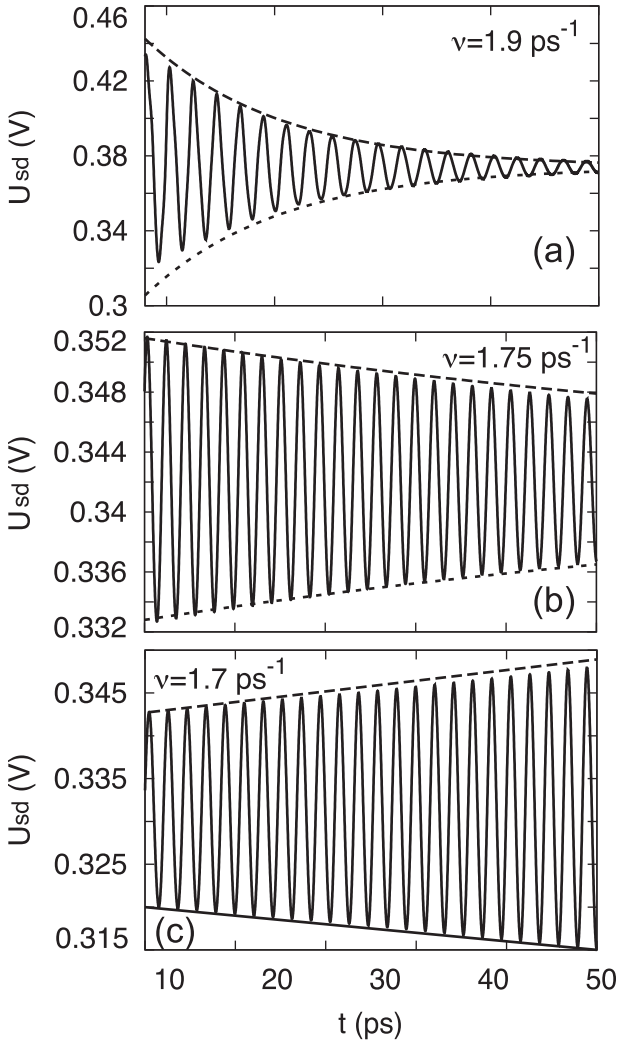

FIG. 5. Calculated source-drain voltages as functions of time for the reported electron velocity relaxation rates $\nu = 1.9$ (a), 1.75 (b) and 1.7 (c) ps^{-1}. Dotted lines represent the envelopes of the time dependent voltages.

to which the relaxation process tends. This state is oscillating in time with a constant increase of the oscillations amplitude (self-oscillation regime). Let us stress that the relaxation processes presented in Fig. 5 are obtained in the absence of any optical beating and the change of the state to which the system relaxes is determined only by processes occurring inside the system.

In this case, we have considered the transition from the stable state into the regime of self-oscillations caused by the change of ν at fixed values of U_g and U_{sd}. A similar transition takes place when U_g and/or U_{sd} are changed at a fixed value of ν. This is illustrated in Fig. 6 which presents the output current-voltage characteristics of the transistor at different values of U_g calculated for $\nu = 2$ ps^{-1} when, under constant voltage U_{sd}, the system is stable. Now, under regime of fixed drain current, the system becomes unstable starting from some threshold value of the current flowing in the HEMT channel (solid line in Fig. 6): in this case, the appearance of plasma self-oscillations leads to self-oscillations of U_{sd}. Below this line, the system is stable and the current-voltage characteristics in both regimes (constant voltage and constant current) coincide. Above the solid line,

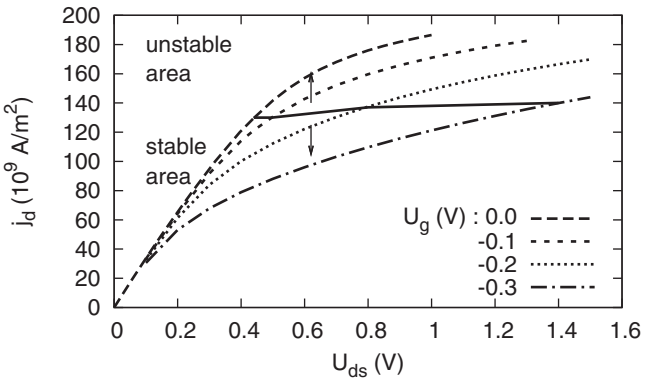

FIG. 6. Calculated drain current as a function of source-drain voltage at different gate voltages U_g. Solid line separates stable and unstable regions for the regime of fixed current flowing in the channel.

there is the instability region where, under the regime of constant applied current, the self-excitation of 2D plasma oscillations takes place. As follows from Fig. 6 in the considered situation, the main critical parameter which controls the transition into the unstable state is the magnitude of the current flowing in the channel. This is illustrated in Fig. 7 which presents the relaxation time of 2D plasma oscillations calculated as a function of the drain current when the latter approaches the instability threshold. Far from the threshold, the relaxation time of plasma oscillations is determined by the velocity relaxation rate in the channel ($\nu \approx 2$ ps^{-1}), while approaching the threshold this relaxation time tends to infinity. As follows from Fig. 7, the transition into the self-oscillations regime exhibits a universal character since it is almost independent of the value of U_g.

Figures 8(a) and 8(b) illustrate a typical pre-threshold behavior of the resonances of ac and dc responses, respectively, induced by photoexcitation at the beating frequency under constant-current operation in the source-drain circuit. Here, the solid line corresponds to the velocity relaxation rate $\nu = 1.75$ (ps)$^{-1}$ (just before the threshold for the Dyakonov-Shur self-oscillations to appear in this situation), while the dashed line calculated at $\nu = 1.9$ (ps)$^{-1}$ illustrates a situation which is still far from self-oscillations. In this example, the transition into the self-oscillation regime takes place for $\nu \lesssim 1.75$ (ps)$^{-1}$ where a clear-cut self-oscillations appear in the simulations (Fig.5(c)). Symbols in Fig. 8(b) correspond to

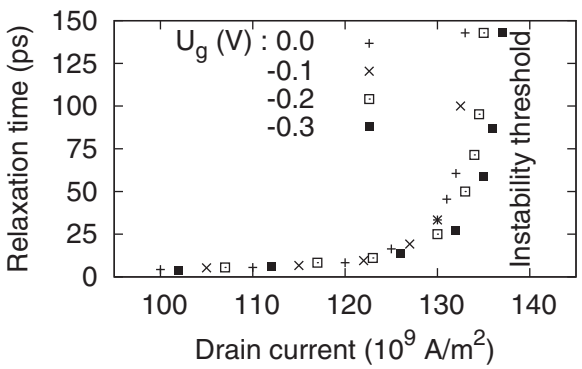

FIG. 7. Calculated relaxation time of 2D plasma excitations as a function of drain current at different gate voltages U_g.

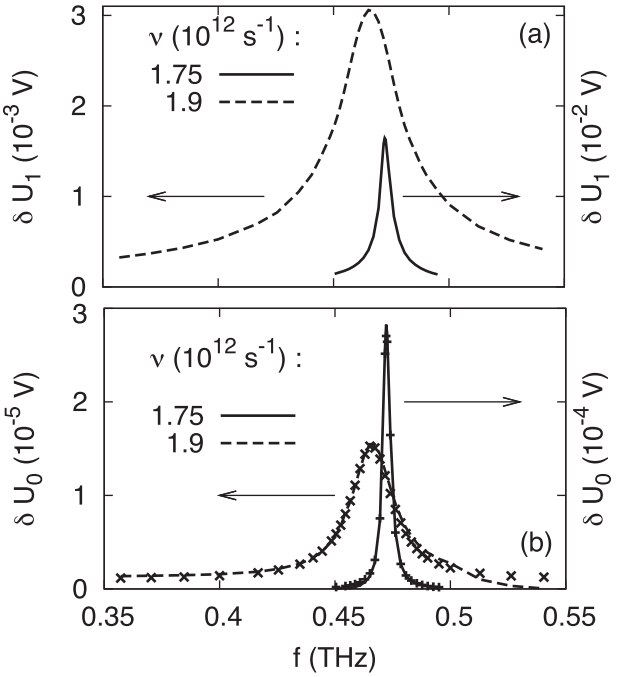

FIG. 8. Calculated amplitudes of the (a) harmonic and (b) average photoresponses of voltage as functions of the beating frequency for the reported values of the velocity relaxation rates.

the square of the ac response amplitude presented in Fig. 8(a) after normalization to the dc resonance maximum. Figure 8(b) fully confirms that the rectification response spectrum $\delta U_0(f)$ is originated by a resonant behavior of the ac components of the response and is related to them by a quadratic dependence. As follows from Fig. 8, the calculations show that, in the pre-threshold regime of the Dyakonov-Shur instability, a small variation (about 10%) of the relaxation rate ν is able to cause a significant variation (about one order of magnitude) of the resonance quality of both ac and dc responses under photoexcitation. These theoretical results are mainly in good agreement with the experimentally observed behavior of the rectification and emission resonances when the system approaches the instability threshold. The significant advantage of the model is that it predicts the same narrowing of the spectrum as we have observed in the experiment. The main disagreement is related to the different directions of the frequency shift of the resonance with increase of the velocity relaxation rate (i.e., the lattice temperature) in the theory and the experiment (see Figs. 4 and 8, respectively).

In accordance with the gradual channel approximation (Eq. (5)), in the channel-under-gate region, the self-consistent electric field magnitude is proportional to the gradient of free-carrier concentration: $E \sim -\frac{\partial n}{\partial x}$. As a result, the presence of carrier stream is always accompanied by a concentration reduction along the stream direction (from the source to the drain ends of the gate). Since the fundamental resonance frequency f_0 depends on the carrier concentration through the relation $f_0 \sim \int_0^L \sqrt{n(x)}dx$, where L is the length of the gated region of the channel (inhomogeneous case), the growth of the gradient, and hence, the reduction of the concentration under the gate, will be accompanied by a red shift of the resonant frequency with respect to the homogeneous case. Indeed,

under the fixed-current operation-mode (i.e., when the drift current $I = e\mu nE$ is constant along the channel), a reduction of the mobility $\mu = e/m\nu$ with increase of ν requires increasing values of $E \sim -\frac{\partial n}{\partial x}$ in order to keep fixed the magnitude of the current I in the channel. As a result, we obtain an increase of the gradient value $-\frac{\partial n}{\partial x}$ and hence, a decrease of the free-carrier concentration under the gate. This leads to the red shift of the plasma resonance frequency under the gate with the increase of the velocity relaxation rate ν.

C. Discussion

The above presented simple HD model demonstrated that a process like the development of the Dyakonov-Shur instability can explain and describe the experimentally observed behavior of the emission and rectification resonances caused by the photo-excitation of 2D plasma waves in the FET/HEMT channels. It is worthwhile to emphasize that the sharp narrowing of the plasma resonances taking place under stationary conditions just before the transition into the self-oscillation regime (obtained here for the Dyakonov-Shur instability) has a general character and it describes the typical scenario of a plasma-instability development independently of its physical nature. It should be stressed that this theoretical model can describe only the stream-plasma instabilities: the Dyakonov-Shur instability which was obtained in the modeling just belongs to this class. Other instabilities related to hot-carrier effects are outside of the present model.

Here, it should be stressed that the effect was observed at values of the source-drain voltage drop $U_{sd} \sim 0.4 - 0.6\,\mathrm{V}$ and at a gate voltage $U_g \geq -0.2\,\mathrm{V}$, when, in principle, one cannot neglect hot-carrier effects such as electron-transfer into upper valleys and impact ionization. In particular, the latter effect explains the increase of the current at $U_{sd} \geq 0.6\,\mathrm{V}$ in Fig. 2. Therefore, the presented experimental results on the resonant radiation emission and rectification effect on the beating frequency under photo-excitation surely evidence the presence of an instability of 2D plasma waves responsible for the observed effect. However, the performed experiments cannot elucidate at present the exact microscopic nature of this instability.

Finally, we remark that the blue shift of the resonant frequency of the fundamental plasma mode with the temperature increase observed in the experiment (while the theoretical model gives the opposite effect) may be interpreted as an evidence of impact ionization processes. Under constant current operation, when the temperature increases, the self-consistent electric field under the gate also increases, thus leading to electrons heating. If the energy threshold for the onset of impact ionization is reached, the temperature increase will be accompanied by an additional increase of the electron concentration under the gate. Such a concentration increase may be responsible for the observed blue shift of the resonant frequency.

V. CONCLUSION

We have demonstrated both experimentally and theoretically the possibility to obtain emission of THz radiations by exciting a HEMT channel by an optical beating. This emission appears to be due to 2D plasma oscillations excited by the photogeneration of electron-hole pairs in the channel and is consequently obtained when the beating frequency is tuned to the first eigenfrequency of 2D plasma waves. In our experiments, such an emission has been observed only at 200 K, when the dynamic behavior of the 2D plasma becomes sufficiently resonant to provide a measurable emission. The spectrum of the emitted radiations is directly related to the spectrum of the excitation; therefore, the studied device may be used as a source of monochromatic THz radiation.

ACKNOWLEDGMENTS

Authors wish to thank T. Gonzalez and J. Mateos (University of Salamanca, Spain) for useful discussions. This work was partially supported by GIS "TeraLab-Montpellier" and by grant No MIP-87/2010 of Lithuanian Science Council.

[1]M. Dyakonov and M. Shur, Phys. Rev. Lett. **71**, 2465 (1993).
[2]A. P. Dmitriev, A. S. Furman, and V. Y. Kachorovskii, Phys. Rev. B **54**, 14020 (1996).
[3]A. P. Dmitriev, A. S. Furman, V. Y. Kachorovskii, G. G. Samsonidze, and G. G. Samsonidze, Phys. Rev. B **55**, 10319 (1997).
[4]W. Knap, J. Lusakowski, T. Parenty, S. Bollaert, A. Cappy, V. V. Popov, and M. S. Shur, Appl. Phys. Lett. **84**, 2331 (2004).
[5]D. Veksler, F. Teppe, A. P. Dmitriev, V. Y. Kachorovskii, W. Knap, and M. S. Shur, Phys. Rev. B **73**, 125328 (2006).
[6]J. Lusakowski, W. Knap, N. Dyakonova, L. Varani, J. Mateos, T. Gonzalez, Y. Roelens, S. Bollaert, A. Cappy, and K. Karpierz, J. Appl. Phys. **97**, 064307 (2005).
[7]N. Dyakonova, A. E. Fatimy, J. Lusakowski, W. Knap, M. I. Dyakonov, M.-A. Poisson, E. Morvan, S. Bollaert, A. Shchepetov, Y. Roelens, C. Gaquiere, D. Theron, and A. Cappy, Appl. Phys. Lett. **88**, 141906 (2006).
[8]Y. M. Meziani, H. Handa, W. Knap, T. Otsuji, E. Sano, V. V. Popov, G. M. Tsymbalov, D. Coquillat, and F. Teppe, Appl. Phys. Lett. **92**, 201108 (2008).
[9]T. Otsuji, Y. Meziani, M. Hanabe, T. Ishibashi, T. Uno, and E. Sano, Appl. Phys. Lett. **89**, 263502 (2006).
[10]V. Gružinskis, R. Mickevicius, J. Pozhela, and A. Reklaitis, Europhys. Lett. **5**, 339 (1988).
[11]A. Mikhailovsky, *Theory of Plasma Instabilities Vol. 1* (Consultants Bureau, New York, 1974).
[12]J. Pierce, J. Appl. Phys. **15**, 721 (1944).
[13]J. Pierce, J. Appl. Phys. **19**, 231 (1948).
[14]B. Ridley and T. Walkins, Proc. Phys. Soc. **78**, 293 (1961).
[15]M. S. Shur, *GaAs Devices and Circuits* (Plenum, New York, 1987).
[16]E. Starikov, P. Shiktorov, and V. Gružinskis, Mater. Sci. Forum **297–298**, 271 (1999).
[17]E. Starikov, P. Shiktorov, V. Gružinskis, L. Varani, C. Palermo, J. Millithaler, and L. Reggiani, J. Phys.: Condens. Matter **20**, 384209 (2008).
[18]L. Landau and E. Lifshitz, *Statistical Physics—Part 1*, Vol. **5** (Pergamon, Oxford, 1980).
[19]M. Lax, Rev. Mod. Phys **38**, 541 (1966).
[20]P. Shiktorov, E. Starikov, V. Gružinskis, L. Reggiani, T. Gonzalez, J. Mateos, D. Pardo, and L. Varani, Phys. Rev. B **57**, 11866 (1998).
[21]P. Shiktorov, E. Starikov, V. Gružinskis, T. Gonzalez, J. Mateos, D. Pardo, L. Reggiani, L. Varani, and J. Vaissiere, Riv. Nuovo Cimento **24**, 1 (2001).
[22]P. Shiktorov, E. Starikov, V. Gružinskis, L. Varani, G. Sabatini, H. Marinchio, and L. Reggiani, J. Stat. Mech.: Theor. Exp. (2009) P01047.
[23]P. Shiktorov, E. Starikov, V. Gružinskis, L. Varani, and L. Reggiani, AIP Conf. Proc. **1129**, 179 (2009).
[24]A. El Fatimy, N. Dyakonova, Y. Meziani, T. Otsuji, W. Knap, S. Vandenbrouk, K. Madjour, D. Theron, C. Gaquiere, M.-A. Poisson, S. Delage, P. Prystawko, and C. Skierbiszewski, J. Appl. Phys. **107**, 024504 (2010).

[25]T. Otsuji, M. Hanabe, and O. Ogawara, Appl. Phys. Lett. **85**, 2119 (2004).
[26]J. Torres, P. Nouvel, A. Akwoue-Ondo, L. Chusseau, F. Teppe, A. Shchepetov, and S. Bollaert, Appl. Phys. Lett. **89**, 201101 (2006).
[27]P. Nouvel, H. Marinchio, J. Torres, C. Palermo, L. Chusseau, D. Gasquet, L. Varani, P. Shiktorov, E. Starikov, and V. Gružinskis, J. Appl. Phys. **106** (2009).
[28]J. Torres, H. Marinchio, P. Nouvel, G. Sabatini, C. Palermo, L. Varani, L. Chusseau, P. Shiktorov, E. Starikov, and V. Gruzhinskis, IEEE J. Sel. Top. Quantum Electron. **14**, 491 (2008).
[29]J.-F. Millithaler, J. Pousset, L. Reggiani, P. Ziade, H. Marinchio, L. Varani, C. Palermo, J. Mateos, T. González, S. Perez, and D. Pardo, Appl. Phys. Lett. **95**, 152102 (2009).
[30]S. Ashmontas, P. Shiktorov, E. Starikov, V. Gruzhinskis, L. Varani, G. Sabatini, and H. Marinchio, AIP Conf. Proc., **1199**, 211 (2010).
[31]H. Marinchio, G. Sabatini, J. Pousset, C. Palermo, J. Torres, L. Chusseau, L. Varani, E. Starikov, and P. Shiktorov, Appl. Phys. Lett. **94**, 192109 (2009).